ELSEVIER

Journal of Alloys and Compounds 330–332 (2002) 760–765

Journal of ALLOYS AND COMPOUNDS

www.elsevier.com/locate/jallcom

A new process for fabrication of metal-hydride electrodes for nickel–metal hydride batteries

S. Zhong*, A. Howes, G.X. Wang, D.H. Bradhurst, C. Wang, S.X. Dou, H.K. Liu

Institute For Superconducting and Electronic Materials, University of Wollongong, Wollongong, NSW 2522, Australia

Abstract

A new method for fabricating a metal-hydride electrode for nickel–metal hydride (Ni–MH) batteries is reported. An expanded copper alloy mesh was used as the electrode substrate to substitute for the conventional nickel foam or nickel-based substrate in order to reduce the cost and increase the processing efficiency. The effects of addition of a dry conductive binder to the electrode active material, the adherence of the electrode active material to the copper-based substrate under pressure and their effects on the open test cells and commercial cells were investigated. Significant improvements to the discharge capacity and life cycle have been achieved by using this new electrode fabrication technique.

Keywords: Ni–MH electrode; Electrode substrate; Alloy mesh; Powder

1. Introduction

The nickel–metal hydride (Ni–MH) battery is one of the most promising battery systems for electric and hybrid vehicle applications [1–4]: its power density and price are very competitive. Commercially available nickel metal-hydride batteries currently use either nickel foam or a nickel-based substrate for the construction of the electrode and the current collector.

A wet-pasting process is generally used for the fabrication of MH electrodes. The metal-hydride powder has to be mixed with a polymer binder and water to make a slurry which is then pasted on to the electrode substrate. A high temperature drying process follows. Severe oxidation can occur during the drying process resulting in lower electrode capacity and shorter electrode service life. Although various methods have been proposed to prevent the oxidation of the electrode active material (EAM), such as using inert atmospheres, they are either not very effective or too expensive [6–8]. This study describes a new method for fabricating an electrode for Ni–MH batteries which aims to eliminate the wet-pasting process by converting the conventional multiple-pasted electrode processes to a complete process thereby eliminating the high temperature and time-consuming drying process. An expanded copper alloy mesh was used as the electrode substrate as a substitute for the conventional nickel foam or nickel-based substrate in order to reduce the cost and increase the processing efficiency. A dry conductive binder was used as a component of the EAM for the enhancement of the conductivity of the electrode and to improve the adherence of EAM to the electrode substrate.

2. Experimental

Nickel-hydride (Ni-H) powder used in this study is a commercially available product of AB_5 type alloys (cerium rich) with a particle size ~30–50 μm. The electrode substrate for the dry powder electrode is a copper (0.05–0.1 wt.%) –indium alloy mesh provided by the Tai-Yi Battery company of China. In order to increase the conductivity, 10 wt.% of nickel powder was added to the Ni-H alloy powder. The alloy powders were then mixed for 3 h using a ball-mill.

Three types of test electrodes were fabricated: (i) conventional wet-pasted electrodes, (ii) dry powder electrodes, and (iii) dry powder electrodes with addition of a conductive binder of 5 wt.% (i.e. a mixture of nickel powder, graphite powder and PTFE powder in the weight ratio 1:1:1).

All three types of electrode substrates were obtained by cutting a copper alloy mesh (for the dry powder electrode) or a nickel mesh (for the wet-pasted electrode) to 20×20-mm size. The wet-pasted electrode was made by mixing

*Corresponding author. Fax: +61-2-4221-5731.
E-mail address: zhong@uow.edu.au (S. Zhong).

0925-8388/02/$ – see front matter
PII: S0925-8388(01)01474-8

the alloy powders with 4 wt.% PTFE or PVA solution. The paste was then applied to both sides of the electrode substrate and compressed under a pressure of 30 MPa. The pasted electrode was then dried in a vacuum desiccator at room temperature for 24 h before testing. For the third type of electrode, 5 wt.% of the dry conductive binder was added to the alloy powders before the ball milling. Both types of dry power electrodes were prepared under a pressure of 60 MPa. The electrochemical measurements were conducted in a half-cell, which consisted of metal hydride as a working electrode, a $NiOOH/Ni(OH)_2$ counter electrode, a commercial separator (a 100% nylon-6 non-woven separator), and a Hg/HgO reference electrode in 6 M KOH solution. For the dry powder electrode, a special polypropylene cell holder was used which enabled a constant pressure to be applied to the electrodes throughout the cell test. The impedance measurements were performed at room temperature using an impedance analyzer (EG&G model 6310). The data were collected as a function of frequency scanned from 100 kHz to 10 MHz and analysed with the aid of an equivalent circuit fitting program. Cyclic voltammetry was performed using an EG&G model 362 scanning potentiostat. Capacity and cycle life tests were performed via an Arbin tester (model $BT4^+$). Both types of commercial sealed cells used in this study were manufactured by Tai-Yi Battery company of China.

3. Results and discussion

All three types of electrodes were activated initially by charging at 30 mA g^{-1} for 20 h, rested for 0.5 h before starting the charge/discharge cycles. The cycle tests were conducted at a charging current density of 120 mA g^{-1} for 3 h and a discharge current density of 120 mA g^{-1} to a cut-off voltage of −0.60 V versus the Hg/HgO electrode. The results are presented in Fig. 1. It can be seen from Fig. 1 that the initial discharge capacities of the three types of working electrodes show different behaviors. The pasted electrode reached its maximum capacity after only four cycles, while the two dry powder electrodes needed approximately ten cycles to approach their maximum capacities.

In contrast to the pasted electrode, the capacity stability was decreased for the dry powder electrode without binder. Following further study on the dry powder pressing process, different methods have been tested for improving the dry powder electrode performance, including the addition of binder to the MH powder. This resulted in a significant improvement in the cycle stability of the electrode as shown in Fig. 1. The increase in the capacity and the cycle stability can be attributed to: (i) the formation and enhancement of electronically conducting bridges within the MH electrode, (ii) the higher compressive force provides better cohesion between the electrode

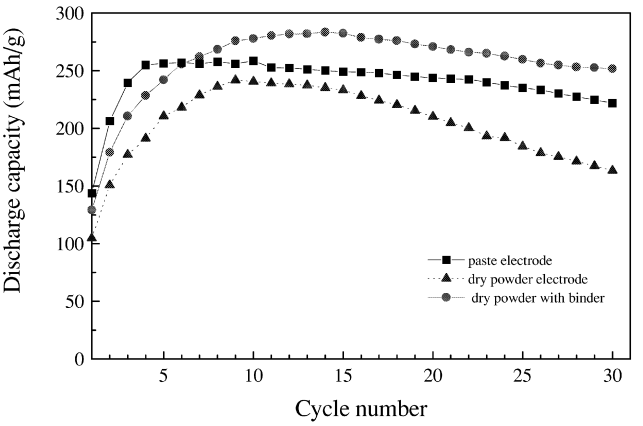

Fig. 1. Discharge capacity versus cycle number for three types of electrodes in open test cells: ■, conventional wet-pasted electrode; ●, the dry powder with conductive binder electrode; ▲, the dry powder electrode without binder.

active material (Ni-H powders) and the copper alloy substrate, resulting in better electronic conductivity and more uniform current distribution, and (iii) formation of a stronger binding between the individual particles.

In order to support the above assumption, impedance analysis was performed during the cycle tests. Fig. 2 shows Nyquist plots of the impedance spectra for the three electrode types. During the first cycle, the cell was charged to 100% state of charge (SOC), held at the open circuit voltage until the working electrode potential was steady and then the impedance spectra were recorded. The Nyquist plots followed a single time-constant model with Warburg impedance at the low frequencies. More data from the Nyquist plots, recorded at the first, fifth and tenth cycles, are presented in Fig. 3. A simplified interfacial model [5] can be used to interpret these experiment results. Both the addition of the conductive binder and the high compression pressure improved the electrode kinetics by lowering the charge-transfer resistance of the reaction process.

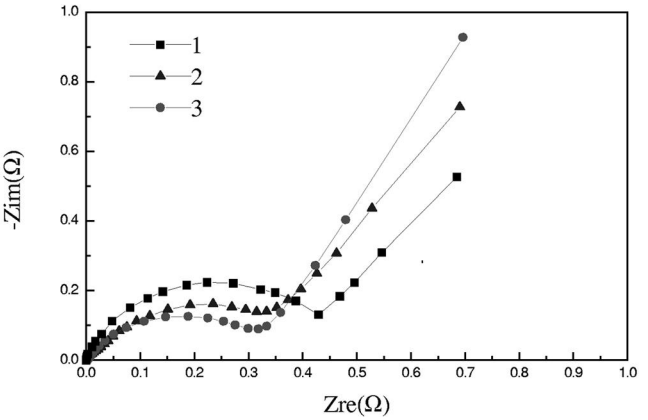

Fig. 2. Nyquist plots of three types of electrodes in open test cells: ■, convectional wet-pasted electrode; ●, the dry powder with conductive binder electrode; ▲, the dry powder electrode without binder.

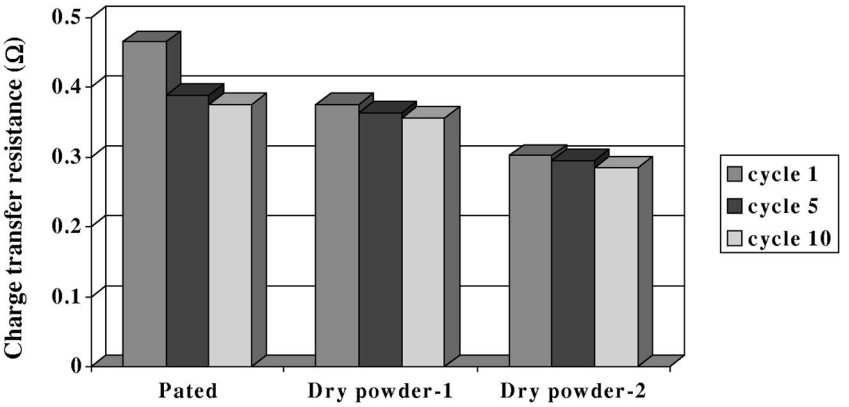

Fig. 3. Charge transfer resistance of three types of electrodes at the first, fifth and 10th cycles.

Cyclic voltammetry (CV) was performed on the dry powder electrodes. The cyclic range was from −1.1 to −0.2 V versus Hg/HgO and the results are presented in Figs. 4 and 5. In the anodic direction, a broad oxidation peak appeared after about ten cycles at approximately −0.65 V and became steady after 100 cycles. This anodic peak was attributed to the oxidation of hydrogen absorbed in the Ni-H electrode. By comparing the two CV plots, it can be seen that the anodic peak current of hydrogen oxidation varied for the two electrodes. The higher anodic peak current obtained from the dry powder electrode with a conductive binder addition implies that the addition of conductive binder to the MH electrode is favorable to the charge–discharge (hydriding–dehydriding) reaction on the electrode. No decomposition of the conductive binder was detected in the CV plots and the conductive binder was therefore considered to be stable in this system.

It has been recognised that the poor cycle life of the test cell, only ~30 cycles as shown in Fig. 1, could be mainly attributed to the open cell construction of the test cells. Therefore, further experiments were performed on sealed commercial AAA type cells with a nominal capacity of 550 mAh. Only two types of commercial cells, a cell with conventional pasted Ni-H electrode and a cell with the dry powder Ni-H electrode with binder additive, were investigated. The fabrication of Ni-H electrodes of these cells was

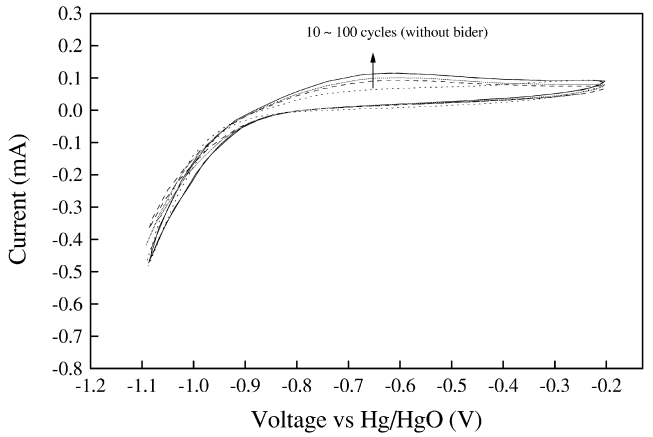

Fig. 4. Cyclic voltammetry (CV) of the dry powder electrode without conductive binder in an open cell.

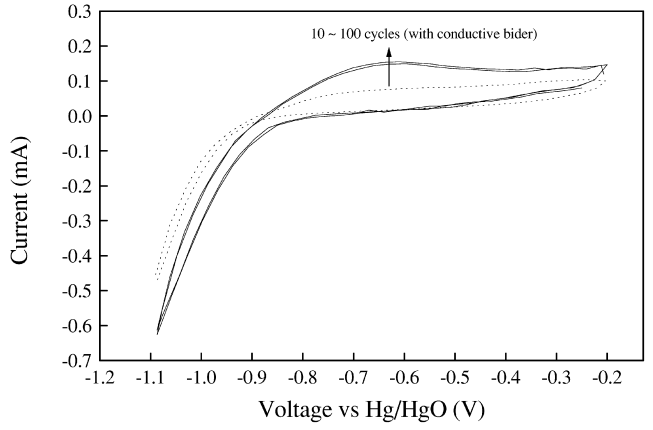

Fig. 5. Cyclic voltammetry (CV) of the dry powder electrode with conductive binder in an open cell.

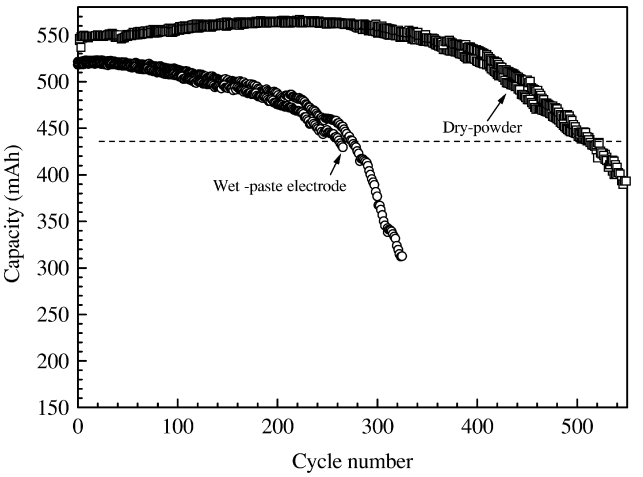

Fig. 6. Discharge capacity versus cycle number, commercial seal cells (AAA type with a nominal capacity of 550 mAh): ○, conventional wet-paste Ni-H electrode; □, dry powder Ni-H electrode with conductive binder.

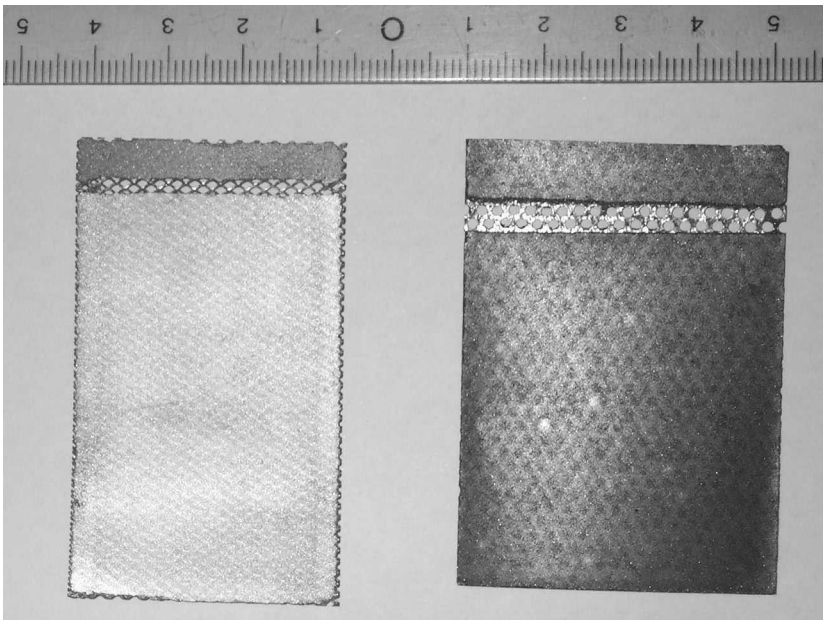

Fig. 7. Left: a dry powder electrode with conductive binder before assembling into a commercial sealed cell. Right: a conventional wet-paste electrode before assembling into a commercial sealed cell.

very close to that of the open cell test electrodes described above. The cycle life tests were performed at 1 C rate charge and 0.2 C rate of discharge to a cut-off voltage of 1.0 V. Results from three types of cells are presented in Fig. 6. The same trends of capacity with cycle number can be found in both Figs. 1 and 6. However, the cycle life was significantly prolonged in these commercial sealed cells. To explore the causes of cell failure, before and after the cycling tests, the commercial cells were disassembled and then analysed. The appearance of the different electrodes before and after the cycle test was compared and is shown in Figs. 7 and 8. It was observed that the active material from the pasted Ni-H electrode dropped off easily from the electrode substrate after cycling. It was considered that negative electrode material drop-off was the main cause for the cell failure. For the pasted electrode, the cell capacity declined to 80% of its original capacity after only ~260 cycles. The appearance of the electrode prepared by the dry pressing process was much more compact than the pasted electrode material as shown in Fig. 9. With the

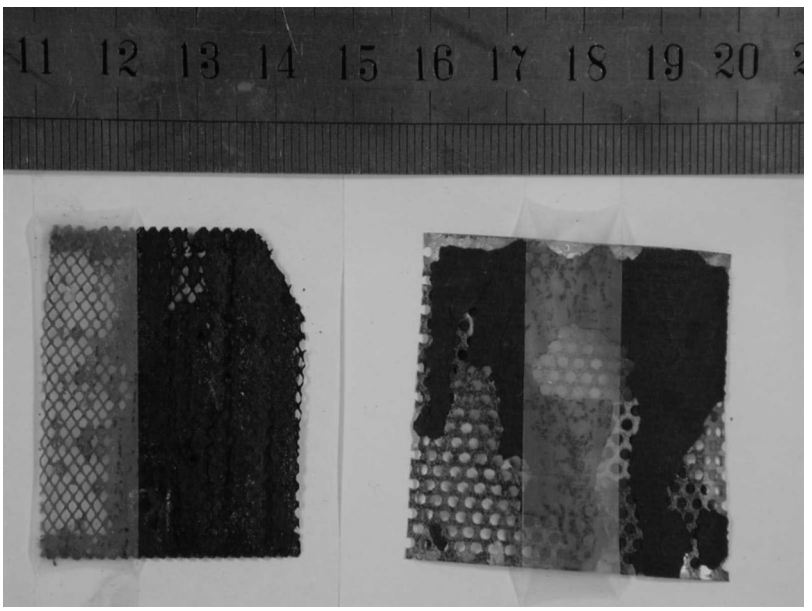

Fig. 8. Left: a dry powder electrode with conductive binder after cycling test (cycled to the end life of the cell, disassembled a commercial sealed cell). Right: a conventional wet-paste electrode after cycling test (cycled to the end life of the cell, disassembled a commercial sealed cell).

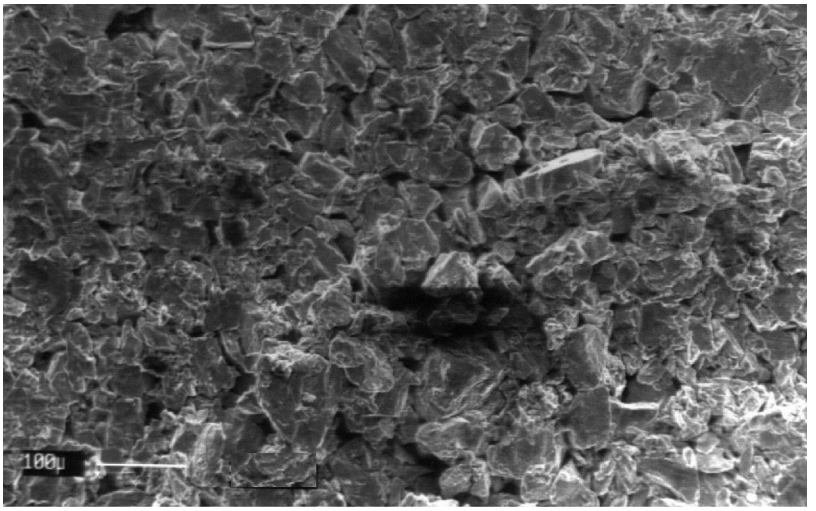

Fig. 9. SEM image of a dry powder Ni-H electrode with addition of a conductive binder before cycling test.

addition of conductive binder, the dry powder compression process significantly increased the coherence between the active material and the electrode substrate. At the end of its service life (~690 cycles), the dry powder compressed electrode was examined by SEM. A loose particle appearance was observed which indicated that the coherence between the metal-hydride particles had decreased as shown in Fig. 10. When viewed in cross-section, obtained by cutting the electrode for the SEM sample preparation, it could be seen that the active material of the compressed electrode was still firmly coherent with the electrode substrate at the end of its service life, as shown in Fig. 8. This kind of coherent force could be attributed to a 'particle inlay' effect. The hard metal-hydride particles could be inlaid into the relatively soft surface of the copper substrate due to the high compressive force used in the preparation process for the dry powder electrode. This 'particle inlay' force is probably much stronger than the particle-to-particle binding force for the pasted type of electrode and could be responsible for the substantial improvements observed in the cell capacity and service life of the dry powder pressed electrodes.

4. Conclusions

A dry pressing method using a copper grid substrate was studied for fabricating a metal-hydride electrode for Ni–MH batteries. Compared with the conventional paste electrode techniques, the dry powder compressed electrode process has the potential to provide a higher processing efficiency and a lower cost of production. Significant improvements in discharge capacity and cycle life have been achieved by using this new electrode fabrication

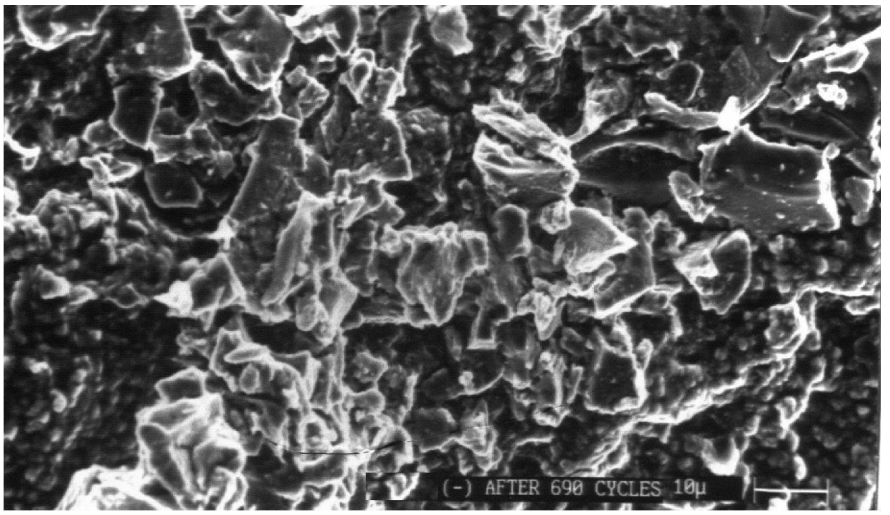

Fig. 10. SEM image of a dry powder Ni-H electrode with addition of a conductive binder after cycling test.

technique. These improvements have been attributed to better adhesion between the electrode active material and the copper-based substrate under the high compression used in the electrode preparation. In order to explore this particle inlay effect, further investigation will be performed on the surface layer of the copper alloy substrate.

References

[1] I. Uehara, T. Sakai, H. Ishikawa, J. Alloys Comp. 253–254 (1997) 641–653.
[2] H.K. Liu, N. Cui, B. Luan, J. Chen, S.X. Dou, D.H. Bradhurst, J. New Mater. Electrochem. Syst. 1 (1998) 77–82.
[3] D. Ilic, M. Kilb, K. Holl, H.W. Praas, E. Pytlik, J. Power Sources 80 (1999) 112–115.
[4] I. Menjak, P.H. Gow, D.A. Corrigan, S. Venkatesan, S.K. Dhar, R.C. Stempel, S.R. Ovshinsky, in: H.A. Frank, E.T. Seo (Eds.), The 13th Annual Battery Conference on Application and Advantages, IEEE, Long Beach, CA, January 1998, 1998, pp. 13–18.
[5] W.L. Zhang, M.P. Kumar, S. Srinivasan, H.J. Ploehn, J. Electrochem. Soc. 142 (1995) 2935.
[6] M. Wolff, M.A. Nuss, et al., US Patent No. 4,820,481 (1989).
[7] S.S. Choi, J.H. Park, UK patent application No. GB 2313561A (1997).
[8] J.S. Wang, S.X. Dou, et al., International Patent Application No. PCT/AU98/01057 (1998).